Title	A small molecule that blocks fat synthesis by inhibiting the activation of SREBP
Author(s)	Kamisuki, Shinji; Mao, Qian; Abu-Elheiga, Lutfi; Gu, Ziwei; Kugimiya, Akira; Kwon, Youngjoo; Shinohara, Tokuyuki; Kawazoe, Yoshinori; Sato, Shin-ichi; Asakura, Koko; Choo, Hea-Young Park; Sakai, Juro; Wakil, Salih J; Uesugi, Motonari
Citation	Chemistry & biology (2009), 16(8): 882-892
Issue Date	2009-08-28
URL	http://hdl.handle.net/2433/112665
Right	© 2009 Elsevier
Type	Journal Article
Textversion	author

A small molecule that blocks fat synthesis by inhibiting the activation of SREBP

Shinji Kamisuki,[1§] Qian Mao,[2§] Lutfi Abu-Elheiga,[2§] Ziwei Gu,[2] Akira Kugimiya,[1] Youngjoo Kwon,[2†] Tokuyuki Shinohara,[1] Yoshinori Kawazoe,[1] Shin-ichi Sato,[2] Koko Asakura,[2] Hea-Young Park Choo,[1†] Juro Sakai,[3] Salih J. Wakil,[2*] and Motonari Uesugi[1,2*]

[1]*Institute for Chemical Research and Institute for Integrated Cell-Material Sciences, Kyoto University, Uji, Kyoto 611-0011, Japan*
[2]*The Verna and Marrs McLean Department of Biochemistry and Molecular Biology, Baylor College of Medicine, Houston, TX 77030, U.S.A.*
[3]*Research Center for Advanced Science and Technology, University of Tokyo, Meguro, Tokyo 153-8904, Japan*

**Correspondence: swakil@bcm.tmc.edu (S.J.W.); uesugi@scl.kyoto-u.ac.jp (M.U.)*

§ Authors contributed equally to the work
† Current address: Ewha Womans University, Seoul 120-750, Korea

RUNNING TITLE

A small molecule that blocks fat synthesis

SUMMARY

Sterol regulatory element binding proteins (SREBPs) are transcription factors that activate transcription of the genes involved in cholesterol and fatty acid biosynthesis. In the present study, we show that a small synthetic molecule we previously discovered to block adipogenesis is an inhibitor of the SREBP activation. The diarylthiazole derivative, now called fatostatin, impairs the activation process of SREBPs, thereby decreasing the transcription of lipogenic genes in cells. Our analysis suggests that fatostatin inhibits the ER-Golgi translocation of SREBPs through binding to their escort protein, the SREBP cleavage-activating protein (SCAP), at a distinct site from the sterol-binding domain. Fatostatin blocked increases in body weight, blood glucose, and hepatic fat accumulation in obese *ob/ob* mice, even under uncontrolled food intake. Fatostatin may serve as a tool for gaining further insights into the regulation of SREBP.

INTRODUCTION

Metabolic syndrome is often ascribed to the long-term intake of excess diets rich in fat or carbohydrates. The amount of fat or carbohydrates in the diets of animals, including humans, contributes significantly to their energy metabolism. Long-chain fatty acids are major sources of energy and important components of the lipids that comprise the cellular membrane (Gibbons, 2003). They are either derived from food or synthesized *de novo* from acetyl-CoA through complex sets of enzymatic reactions— namely, lipogenesis—that involve the conversion of glucose into acylglycerides (Gibbons, 2003; Wakil, 1989). These reactions include glycolysis and the citric acid cycle, which collectively lead to the formation of the backbone carbons of fatty acids and glycerols for the synthesis of lipids.

Transcription factors SREBP-1a, SREBP-1c, and SREBP-2 are major regulators of genes encoding enzymes in lipogenic pathways (Brown and Goldstein, 1997; Osborne, 2000). SREBPs are synthesized as ER-membrane-bound precursors; they must be proteolytically released by two proteases bound to the Golgi membrane, Site-1 (S1P) and Site-2 (S2P) proteases, to generate an active form that activates transcription of target genes in the nucleus (Brown and Goldstein, 1997; Sakai et al., 1996). The proteolytic activation of SREBPs is tightly regulated by sterols through interaction with the SREBP cleavage-activating protein (SCAP), an ER-membrane-bound escort protein of SREBPs (Goldstein et al., 2006; Hua et al., 1996). When sterols accumulate in the ER membranes, the SCAP/SREBP complex fails to exit the ER to the Golgi apparatus, and the proteolytic processing of SREBPs is suppressed. Thus, SREBPs are key lipogenic transcription factors that govern the homeostasis of fat metabolism.

We previously discovered a small organic molecule, formerly called 125B11, that we now call fatostatin (Figure 1A); this molecule inhibited the insulin-induced adipogenesis of 3T3-L1 cells and the serum-independent growth of human androgen-independent prostate cancer (DU145) cells (Choi et al., 2003). Results of the present study show that fatostatin blocks the activation of SREBPs in cells in tissue culture. Furthermore, we show that fatostatin reduced adiposity, ameliorated fatty liver by reducing triglyceride (TG) storage, and lowered hyperglycemia in *ob/ob* mice.

RESULTS

Fatostatin reduces expression of SREBP-responsive genes

To gain information about specific molecular pathways affected by fatostatin, gene expression profiles of drug-treated and untreated cells were compared. DU145 cells were treated with fatostatin or DMSO alone, and the extracted mRNA samples were analyzed by Affymetrix DNA microarrays mapping 33,000 genes. Of these genes, transcription levels of 63 genes decreased at least 35% in response to fatostatin treatment (Figure S1). Thirty-four of the affected genes—such as those encoding biosynthetic enzymes—were directly associated with fat or sterol synthesis; 18 of the affected genes have been reported to be controlled by SREBPs (Horton et al., 2003). Downregulation of the affected SREBP-responsive genes was confirmed by RT-PCR experiments (Figures 1B and 1C). The high occurrence among the downregulated genes of the known SREBP-responsive genes and fat/cholesterol biosynthesis genes implies that fatostatin acts either directly or indirectly on the SREBP pathway.

Fatostatin blocks proteolytic activation of SREBPs

To confirm that fatostatin acts on the SREBP pathway, the ability of endogenous SREBPs to activate the transcription of an SREBP-responsive reporter gene was measured in Chinese hamster ovary-K1 (CHO-K1) cells in either the presence or the absence of fatostatin. Fatostatin decreased activation of the reporter gene, in which the expression of luciferase is controlled by three repeats of sterol regulatory elements (SREs) (pSRE-Luc, Figure 1D). We also analyzed the effects of fatostatin on gene activation by an exogenously expressed mature form of SREBP-1 (amino acids 1-436), a constitutively active form of SREBP. Fatostatin had a limited effect on the ability of the mature form of SREBP to activate the reporter gene (Figure 1E). Collectively, these results suggest that fatostatin impairs the activation process of SREBPs.

To determine if fatostatin affects the ER-Golgi translocation and proteolytic processing of SREBPs, we used a reporter assay developed by Sakai et al. (1998). In this assay a secreted alkaline phosphatase, fused with an SREBP-2 fragment lacking the NH_2-terminal DNA-binding domain (PLAP-$BP2_{513–1141}$), permits monitoring of translocation and processing through changes in the fluorescence of a fluorogenic phosphatase substrate (Figure 1F). When cells were co-transfected with plasmids encoding PLAP-$BP2_{513–1141}$ and SCAP, PLAP phosphatase was secreted and fluorescence signals were generated. Secretion was similarly decreased by the addition of either fatostatin or sterols (Figure 1F). The fatostatin-mediated inhibition of SREBP activation was confirmed by western blot analysis of SREBPs. Treatment of the CHO-K1 cells with fatostatin decreased the amount of the 68

KDa mature nuclear active form N of SREBP-2 and increased the amount of the 125 KDa precursor form P of SREBP-2 (Figure 1G). Similar results were obtained for SREBP-1; the nuclear active form N is reduced in the presence of fatostatin (Figure S2). These results collectively suggest that fatostatin blocks the activation process of both isoforms of SREBP.

Fatostatin inhibits translocation of SCAP from ER to Golgi apparatus

We hypothesized that fatostatin impairs either the proteolytic cleavage of SREBPs in the Golgi apparatus or the ER-to-Golgi translocation of the SCAP/SREBP complex. Brefeldin A, a natural product that blocks anterograde movement of proteins from the ER to the Golgi, is known to render SREBPs unresponsive to sterols; it causes SREBPs to be constitutively processed in the ER by relocating S1P from the Golgi to the ER (DeBose-Boyd et al., 1999). In the presence of brefeldin A, fatostatin like sterols had no impact on the SREBP processing as shown by the formation of the proteolytic products (N) in the CHO-K1 cells (Figure 2A), suggesting that fatostatin does not block the proteolysis itself.

The translocated SCAP has higher levels of glycosylation, and it is more resistant to endoglycosidase H than ER-bound SCAP. Inhibiting the ER to Golgi translocation of SCAP by sterols increases the sensitivity of SCAP to endoglycosidase H (Figure 2B) (Nohturfft et al., 1998). To determine whether fatostatin blocks the ER-to-Golgi translocation of the SCAP/SREBP complex, thus increasing SCAP sensitivity to endoglycosidase H, we analyzed the extent of N-linked glycosylation of SCAP in the Golgi apparatus. Cells were grown in the absence or presence of fatostatin or sterols, and membrane fractions were treated successively with trypsin and endoglycosidase H. In cells

grown without fatostatin and sterols, a tryptic fragment of SCAP was more resistant to endoglycosidase H and had one or two saccharide chains (Figure 2C**,** lane 1). In contrast, when cells were grown in the presence of fatostatin or sterols the SCAP fragment was less resistant to endoglycosidase H and had either zero or one saccharide chain (Figure 2C**,** lanes 2 and 3). Therefore fatostatin, like sterols, appears to inhibit the translocation of SCAP from the ER to the Golgi.

Fatostatin interacts with SCAP

Studies of the relationship of structure and activity in fatostatin indicated that this molecule retains or even increases biological activity when its toluene moiety is modified with a variety of alkyl or aryl sulfonamide groups (unpublished data). One fluorescent derivative, dansyl fatostatin (Figure 3A), retained the ability to block SREBP activation (Figure S5) and served as a microscopic probe. Confocal microscopic analyses revealed that the localization of dansyl fatostatin overlapped with that of ER-tracker red, a specific marker for ER (Figure 3B). In contrast, the control dansyl molecule—which lacked fatostatin—failed to localize to any organelle (data not shown). The selective ER localization implies that fatostatin binds to a protein in the ER; the most likely candidate is SCAP, the target of cholesterol for the control of SREBP (Radhakrishnan et al., 2004). To test this hypothesis, proteins bound to a fatostatin-polyproline linker-biotin conjugate (Figure 3A) (Sato et al., 2007) were purified from cell lysates and analyzed by western blots with antibodies against SCAP, SREBP-1, SREBP-2, and HMG-CoAR, as well as ATF6, an unrelated ER-bound transcription factor (Ye et al., 2000). The results suggest that

fatostatin binds directly or indirectly to SCAP (Figure 3C). The interaction was impaired by adding excess amounts of fatostatin but not cholesterol (Figure 3D). The conjugate **4** that lacks fatostatin failed to bind to SCAP (Figure 3C).

In order to examine whether fatostatin interacts with SCAP directly or not, we synthesized a fatostatin derivative coupled with a photo-active diazirine group and a biotin molecule (conjugate **5**, Figure 4A). This fatostatin conjugate is still as active as fatostatin in reporter gene assays (Figure S5) and allows covalent crosslinking of the biotinylated molecule with its target protein upon UV irradiation. FLAG-tagged full-length SCAP protein (amino acids 1-1276) was expressed in human embryonic kidney (HEK) 293T cells and immunopurified with a FLAG antibody. The partially purified SCAP protein was incubated with conjugate **5** and irradiated by UV to allow crosslinking. The western blot analysis of the products using streptavidin-HRP or a FLAG antibody showed a biotinylated protein band whose electrophoretic mobility matches that of full-length SCAP (Figure 4B). Without UV irradiation, this band was undetectable (Figure S6), indicating that the interaction of fatostatin with SCAP is reversible. A FLAG-tagged NH_2-terminal fragments of SCAP (amino acids 1-415 and 1-448), which include a binding site for sterols, failed to crosslink to fatostatin conjugate **5** (Figure 4B). These results suggest that fatostatin directly interacts with SCAP at a site distinct from the sterol-binding domain.

Sterols are known to induce the interaction of SCAP with ER-bound INSIG proteins, thereby inhibiting the exit of SCAP from ER (Yang et al., 2002; Yabe et al., 2002). To examine if fatostatin similarly induces the SCAP-INSIG interaction, we performed coimmunoprecipitation experiments with cells expressing Myc-tagged INSIG-1. The

results showed that Myc-tagged INSIG-1 binds SCAP in the presence of sterols but not in the presence of fatostatin, even at high concentrations (Figure 5). These results suggest that both sterols and fatostatin modulate the function of SCAP, but their mechanisms may be distinct from each other.

One remaining possibility is that fatostatin may inhibit the interaction of SCAP with SREBPs. We examined if conjugate **5** binds to a COOH-terminal domain of SCAP (amino acids 732-1276) which includes SREBP-binding domain (Sakai et al., 1998). The results showed that conjugate **5** failed to interact with the COOH-terminal domain of SCAP whereas the other half of SCAP (amino acids 1-767) reacted with conjugate **5**. Consistent with this observation, when we conducted coimmunoprecipitation experiments with HSV-tagged SREBP-2 (Figure S7), fatostatin had no impacts on the binding between SREBP-2 and SCAP.

Effects of fatostatin on *ob/ob* mice--body weight, blood constituents, and liver and adipose tissues

Having established a key role of SREBPs in lipogenesis, we then examined the pharmacological effects of fatostatin on *ob/ob* mice, a mouse model of obesity with uncontrolled food intake. Fatostatin was delivered intraperitoneally daily for 28 days, and food intake and body weight were monitored. The average daily food intake of the treated mice was not significantly different from that of the controls (5.4 ± 1.5 vs. 5.9 ± 1.4 g/mouse/d, respectively), and no obvious toxicity was observed during the treatment (Figures 6A and 6B). Following four weeks' treatment with fatostatin, the mice weighed

approximately 12% less than the untreated controls (32.1 $\pm$ 1.4 and 36.2 $\pm$ 2.2 g/mouse, respectively, p = 0.02). One of the most distinct phenotypes in *ob/ob* mice is hyperglycemia resulting from insulin resistance. Examination of blood constituents (Figure 6C) revealed that the average glucose levels of the treated mice was ~70% lower than that of the untreated mice (153.2 $\pm$ 30.5 vs. 429.4 $\pm$ 87 mg/dl, respectively, p = 0.003), which is in the range of normal glucose levels. These results are consistent with the reported role of SREBP-1c in the pathogenesis of hepatic insulin resistance (Ide et al., 2004).

The serum level of total cholesterol showed a lower trend in fatostatin-treated mice than in the control mice (183 ± 16 vs. 219 ± 18 mg/dl, respectively) (P = 0.06). However, there was a significant decrease of approximately 35% in LDL (31 ± 3 mg/dl vs. 48 ± 8 mg/dl, respectively) and a lesser decrease of approximately 22% in HDL (144 ± 11 mg/dl vs. 183 ± 12 mg/dl, respectively) for the fatostatin-treated mice compared with the control mice. Because there was a greater decrease in the LDL serum levels than in the HDL serum levels of the fatostatin-treated mice, this may be a desirable outcome following treatment with fatostatin. The serum level of TGs increased approximately 30% (115 ± 11 mg/dl vs. 79 ± 12 mg/dl, respectively) in the fatostatin-treated mice compared with the control mice, suggesting that fatostatin increases secretion and mobilization of TG from the liver. The level of VLDL, which transports TGs, phospholipids, and cholesterol—and which is calculated according to TG levels—increased approximately 50% (23.1 ± 2.31 mg/dl vs. 15.8 ± 2.42 mg/dl, respectively) (Figure 6C). It should be noted that mice are a poor model to investigate pharmacological effects on cholesterol levels as statins generally are not effective in reducing cholesterol levels in mice.

The serum level of the non-esterified fatty acids (NEFA) was approximately 70% higher in the fatostatin-treated mice compared with the control mice (1.93 ± 0.261 mEq/l vs. 0.7 ± 0.2 mEq/l, respectively) (Figure 6C). This increase in NEFA levels may be caused by increased lipolysis from adipose tissue, in response to an increased demand for fatty acid oxidation. NEFA is known to be associated with insulin resistance in both animals and human. Although the serum levels of NEFA were elevated in the fatostatin-treated mice, the glucose levels were significantly lower than in the control mice, suggesting an improvement in insulin sensitivity. It is interesting that ketone bodies (β-hydroxybutyrate) increased approximately seven fold in the fatostatin-treated mice compared with the control mice (3.62 ± 1.41 mg/dl vs. 0.5 ± 0.37 mg/dl, respectively (Figure 6C). The high levels of ketone bodies in the fatostatin-treated mice suggest a significant increase in fatty acid oxidation in the livers. We have also recently shown that increased fatty acid oxidation in liver, adipose, and muscle tissues in acetyl-CoA carboxylase 2 ($Acc2^{-/-}$) mutant mice resulted in increased NEFA as well as higher ketone bodies in the blood (Abu-Elheiga et al., 2001; Abu-Elheiga et al., 2003; Oh et al., 2005).

Another phenotype of *ob/ob* mice is excessive accumulation of fat in organs, including non-alcoholic fatty liver. Livers in the control *ob/ob* mice were enlarged, and their pale color was evidence of fat; the livers of the mice treated with fatostatin appeared normal (Figure 7A). Livers of the treated mice averaged approximately 32% lower in weight, and fat pads were smaller, than those of the control mice (Figure 7B). Oil Red-O section staining showed that the livers of the control mice contained abundant lipid droplets; in contrast, the livers of the treated mice contained lower levels of lipid

accumulation (Figure 7C). The TG and cholesterol levels in the livers of the treated mice were also reduced (Figure 7D). The prevention of fatty liver by fatostatin in *ob/ob* mice is in agreement with the reported role of SREBP-1 in developing fatty liver: Transgenic mice overexpressing SREBP-1 developed fatty livers (Horton et al., 2003), while *ob/ob* mice lacking SREBP-1 (*lep*$^{ob/ob}$ *X Srebp 1*$^{-/-}$) had healthy livers (Yahagi et al., 2002).

The reduction of hepatic fat levels in the fatostatin-treated mice was considered to be due to a decreased hepatic expression of SREBP-responsive lipogenic enzymes. Therefore, we examined the effects of fatostatin on the hepatic protein levels and enzymatic activities of representative SREBP-responsive lipogenic enzymes, including FAS, ACC, stearoyl-CoA desaturase 1 (SCD1), and ATP citrate lyase (ACL). Biochemical analyses showed that protein levels and activities of the lipogenic enzymes were reduced in liver extracts of fatostatin-treated mice (Figures 7E, 7F, and 7G). The decrease in protein levels can be attributed to a decrease in transcriptional or translational regulation. We used real time PCR and determined the levels of mRNA of representatives of lipogenic genes ACC1, FAS, SCD1, HMG-CoA reductase (HMG-R), LDL receptor (LDLR) and mevalonate pyrophosphate decarboxylase (MVD). There was a reduction in the mRNA levels of these genes (Figure 7H). These results, which are consistent with lower levels of enzyme proteins and activities, indicate that fatostatin lowers lipogenesis by inhibiting the maturation of SREBP. It appears that fatostatin blocks the processing of SREBP in liver, downregulates lipogenic enzymes, and reduces hepatic TG storage.

DISCUSSION

Modulation of the SREBP pathway by small molecules is not new. Researchers at GlaxoSmithKline have discovered small molecules that activate SCAP/SREBP proteins and lower blood cholesterol levels through the increased expression and activity of the LDL receptor (Grand-Perret et al., 2001). Nevertheless, fatostatin represents the first non-sterol-like synthetic molecule that inhibits the activation of SREBPs. Both fatostatin and the GlaxoSmithKline molecules appear to modulate the function of SCAP/SREBP complex, resulting in distinct impacts on the fatty acid and/or cholesterol metabolism of experimental animals. SCAP may be a key protein that is amenable to both positive and negative control with simple synthetic molecules.

Our results of binding and crosslinking studies suggest that fatostatin binds to SCAP at a distinct site from the sterol-binding domain previously reported by Goldstein and co-workers (Adams et al., 2004). The fatostatin's mechanism for the modulation of the SREBP-escorting function of SCAP is likely to be distinct from that of sterols: the binding site of fatostatin in SCAP is different from that of sterols, and the interaction does not induce the SCAP-INSIG interaction. Further studies are needed to determine the complete mechanism of action of fatostatin. One possibility is that fatostatin may induce the interaction of SCAP with unknown ER proteins other than INSIGs. Alternatively, fatostatin may directly affect the interaction of SCAP with COPII proteins, which cluster the SCAP-SREBP complex into coated vesicles that exit from the ER and travel to the Golgi (Espenshade et al., 2002). PI3 kinase inhibitors have been shown to inhibit ER-to-Golgi transport of SCAP (Du et al., 2006). To test whether fatostatin acts through Akt to control

SCAP transport, we conducted a western blot analysis with anti-phospho-Akt antibody. Our data suggested that fatostatin has no effect on phosphorylation of AKT (data not shown).

Fatostatin was originally discovered in our laboratory as a small molecule that generates two distinct phenotypes in cultured mammalian cells: inhibition of the insulin-induced adipogenesis of 3T3-L1 mouse fibroblast cells; and repression of the serum-independent growth of DU145 human prostate cancer cells. The first phenotype is in complete agreement with our conclusion that fatostatin is a blocker of SREBPs because of the known role of SREBP-1 in lipogenesis. The second effect of fatostatin on the serum-independent growth may also be consistent with the inhibition of SREBPs, because the serum-free medium lacks external fat sources. Without exogenous lipid present in the serum, cells need to synthesize fatty acids and cholesterol, the building blocks of membranes, to maintain the cell growth. To test the importance of lipids in the cell growth, the growth of the SREBP-1 knockdown cells was monitored in a fat free serum medium. The SREBP-1 silencing impaired the cell growth in a fat-free medium as much as it did in the serum-free IGF1-containing medium (Figure S8). These observations suggest that fatostatin blocks the serum-independent growth of cancer cells through the inhibition of SREBP-1.

To evaluate and validate the effectiveness of fatostatin *in vivo*, and possibly identify other desirable phenotypes produced by this small molecule, we studied its effect on an *ob/ob* obese mouse model. An important discovery in the fatostatin treated mice was a reduction of both body weight and blood glucose (Figure 6). The reduced body weight may be caused by a lower lipogenesis rate, as a result of the downregulation of lipogenic

enzymes such as ACC, FAS, ACL, and SCD1. Expression and activities of these enzymes were significantly downregulated in fatostatin treated mice, which resulted in lower levels of long-chain fatty acid derivatives in their livers. In addition, the reduction in malonyl-CoA—the product of ACC and a potent inhibitor of carnitine palmitoyl transferase—may result in enhanced fatty acid oxidation and fat burning. We have shown previously that $Acc2^{-/-}$ mutant mice are lean and exhibit a higher rate of fatty acid oxidation in muscle, liver, and adipose tissue, and they have lower blood glucose levels (Abu-Elheiga et al., 2001; Abu-Elheiga et al., 2003; Oh et al., 2005). Similar metabolic profiles have been observed with peroxisome proliferator-activated receptor (PPAR) ligand treatment (Cho et al., 2008). We tested whether fatostatin can serve as a ligand for PPARs (α, γ and δ). The results showed that fatostatin failed to activate either PPAR at detectable levels as compared with known PPAR ligands (Figure S9).

Our animal results support the notion that inhibition of SREBPs by fatostatin downregulates lipogenic enzymes, enhances fatty acid oxidation, reduces weight, and increases insulin sensitivity, which causes a lower level of glucose. Fatostatin or its analogs, therefore, may serve as a chemical tool which provides insights into the SCAP-mediated regulation of the SREBP pathway. Fatostatin, or its analogs, may also become seed molecules for pharmacological intervention in the metabolic syndrome. It should be noted, however, that further studies with transgenic animals may be needed to claim that the mechanism of fatostatin *in vivo* is the same as that in cultured cells.

SIGNIFICANCE

Fatostatin represents the first non-sterol-like synthetic molecule that inhibits the activation of SREBPs, transcription factors that play central roles in lipogenesis. Uncontrolled lipogenesis is implicated in a number of metabolic diseases, including diabetes and cardiovascular diseases. Major efforts are being devoted to target different players in the fat metabolism. Fatostatin or its analogs may serve a tool for gaining further insights into the regulation of SREBP and fat metabolism.

EXPERIMENTAL PROCEDURES

Cell culture

CHO-K1 cells were maintained in a Dulbecco's modified Eagle's medium/Ham's F12 medium [1:1] with 5% fetal bovine serum, 100 units/mL penicillin, and 100 μg/mL streptomycin sulfate at 37°C under 5% CO_2. Human androgen-independent prostate cancer (DU145) cells were maintained in an Eagle's minimum essential medium containing 2 mM L-glutamine, 1.0 mM sodium pyruvate, 0.1 mM nonessential amino acids, and 1.5 g/L sodium biocarbonate with 10% fetal bovine serum, 100 units/mL penicillin, and 100 μg/mL streptomycin sulfate at 37°C under 5% CO_2. 293T cells were maintained in a Dulbecco's modified Eagle's medium with 10% fetal bovine serum, 100 units/mL penicillin, and 100 μg/mL streptomycin sulfate at 37°C under 5% CO_2

RT-PCR experiments

Total RNA was extracted from DU145 cells in TRI reagent (Molecular Research Center) and isolated with an RNeasy Mini Kit (Qiagen). The RNA sample was subjected to RT-

PCR by using the Access RT-PCR System (Promega). RT-PCR reactions contained total RNA, 1 μM of each primer, 0.2 mM dNTP, 1 mM $MgSO_4$, AMV reverse transcriptase (2 units), and *Tfl* DNA polymerase (2 units) in a final volume of 25 μL. The primer pairs used were as follows: 5'-TCA GAC CGG GAC TGC TTG GAC GGC TCA GTC -3' and 5'-CCA CTT AGG CAG TGG AAC TCG AAG GCC G -3' for Low density lipoprotein receptor (LDLR); 5'- GCC TGC TTG ATA ATA TAT AAA C -3' and 5' - CAC TTG AAT TGA GCT TTA G -3' for stearoyl-CoA desaturase (SCD1); 5' -AAG AAA AAG TGT CAG ACA GCT GG -3' and 5' - TGG ACT GAA GGG GTG TTA GC -3' for ATP citrate lyase (ACL); 5'- GCC CGA CAG TTC TGA ACT GGA ACA -3' and 5'- GAA CCT GAG ACC TCT CTG AAA GAG -3' for 3-hydroxy-3-methylglutaryl-CoA reductase (HMG-CoAR); 5'- CTG CCT GAC TGC CTC AGC -3' and 5'- ACC TCT CCT GAC ACC TGG G -3' for mevalonate pyrophosphate decarboxylase (MVD); 5'-AAG ACT TCA GGG TAA GTC ATC A-3' and 5'- CGT GTA TAA TGG TGT CTA TCA G -3' for insulin induced gene 1 (INSIG1). The amplification conditions were as follows: 1 cycle at 94°C for 4 min, then denatured at 94°C for 40 s, annealed at 50°C for 40 s, and extended at 68°C for 2 min with 22 cycles for SCD1 and HMG CoAR, annealed at 58°C with 24 cycles for LDLR and INSIG1, or annealed at 60°C with 24 cycles for ACL, annealed at 55°C with 30 cycles for MVD. The amplified DNAs were analyzed by an agarose gel and quantified with the Scion-image software.

Luciferase reporter assay

On day 0, CHO-K1 cells were plated out onto a 96-well plate in medium A (a 1:1 mixture of Ham's F-12 medium and Dulbecco's modified Eagle's medium, with 5% fetal bovine serum, 100 units/mL penicillin, and 100 μg/mL streptomycin sulfate). On day 2, the cells were transiently co-transfected with pSRE-Luc (an SRE-1-driven luciferase reporter construct) (Hua et al., 1995) and pAc-β-gal (β-gal reporter in which the expression of β-gal is controlled by an actin promoter), using Lipofectamine reagent (Invitrogen). After incubation for 5 hrs the cells were washed with phosphate-buffered saline (PBS) and then incubated, in the absence or presence of fatostatin, in medium B (a 1:1 mixture of Ham's F-12 medium and Dulbecco's modified Eagle's medium, with 5% lipid-depleted serum, 100 units/mL penicillin, 100 μg/mL streptomycin sulfate, 50 μM compactin, and 50 μM sodium mevalonate). After 20 hrs of incubation the cells in each well were lysed, and aliquots were used to measure luciferase and β-galactosidase activities. Luciferase activity was normalized by the activity of β-galactosidase. For overexpression of the N-terminal matured form of SREBP-1c, pCMV-SREBP-1c(1-436) was co-transfected with pSRE-Luc and pAc-β-gal.

PLAP-BP2 cleavage

On day 0, CHO-K1 cells were plated out onto a 96-well plate in medium A. On day 2, the cells were transiently co-transfected with pCMV-PLAP-BP2(513–1141), pCMV-SCAP and pAc-β-gal, using Lipofectamine reagent (Invitrogen). After incubation for 5 hrs the cells were washed with PBS and then incubated in medium B, in the absence or presence of fatostatin (20 μM) or sterols (10 μg/mL cholesterol and 1 μg/mL 25-hydroxycholesterol).

After 20 hrs of incubation, an aliquot of the medium was assayed for secreted alkaline phosphatase activity. The cells in each well were lysed, and used for measurement of β-galactosidase activities. The alkaline phosphatase activity was normalized by the acitivity of β-galactosidase.

Western blot analysis of SREBP processing

On day 0, CHO-K1 cells were plated out onto a 100 mm dish of medium A. On day 2, the cells were washed with PBS, and then incubated in medium B in the absence or presence of fatostatin. On day 3, the cells were washed once with cold PBS, and then treated with buffer containing 10 mM Tris-HCl, pH 7.6, 100 mM NaCl, 1% (w/v) SDS, and protease inhibitor mixture (1 μg/mL pepstatin A, 10 μg/mL leupeptin, and 200 μM phenylmethylsulfonyl fluoride). The protein concentration of each total cell extract was measured (BCA kit; Pierce), after which a 22-33 μg aliquot of cell extract was mixed with 0.25 volume of buffer (250 mM Tris-HCl, pH 6.8, 10% SDS, 25% glycerol, 0.2% (w/v) bromophenol blue, and 5% (v/v) 2-mercaptoethanol) and heated for 7 min at 95°C. The samples were separated on a 10% SDS-PAGE gel and blotted, using mouse monoclonal antibodies against SREBP-2 (IgG-7D4) (Yang et al., 1995) or SREBP-1 (IgG-2A4) (Sato et al., 1994). The specific bands were visualized using enhanced chemiluminescent (ECL) detection reagents (Amersham).

Preparation of cell membrane fraction

Cells were harvested, and then resuspended in buffer containing 10 mM Hepes-KOH (pH 7.4), 10 mM KCl, 1.5 mM $MgCl_2$, and 1 mM sodium EDTA, then passed through a 22-gauge needle and centrifuged at 1,000 × *g* for 5 min. The postnuclear supernatants were then centrifuged at 10^5 × *g* for 30 min, and the supernatant was removed.

Modification of SCAP oligosaccharides

The membrane fraction of cell lysates was resuspended in 0.1 mL of buffer containing 10 mM Hepes·KOH (pH 7.4), 10 mM KCl, 1.5 mM $MgCl_2$, 1 mM sodium EDTA, and 100 mM NaCl. Aliquots of protein were then incubated in the absence or presence of 1 μg of trypsin, in a total volume of 58 μL, for 30 min at 30°C. Reactions were stopped by the addition of 2 μL (400 units) of soybean trypsin inhibitor. For subsequent treatment with endoglycosidase H, individual samples received 10 μl of solution containing 3.5% (wt/vol) SDS and 7% (vol/vol) 2-mercaptoethanol. After heating at 100°C for 10 min, each sample received sequential additions of 9 μl of 0.5 M sodium citrate (pH 5.5), 5 μL of solution containing 17× protease inhibitors (a concentration of 1×, corresponding to 10 μg/mL leupeptin, 5 μg/mL pepstatin A, and 2 μg/mL aprotinin), and 1 μL (5 units) of endoglycosidase H. The reactions were carried out overnight at 37°C, then stopped by the addition of 20 μL of buffer containing 0.25 M Tris-HCl (pH 6.8), 2% SDS, 10% (vol/vol) glycerol, 0.05% (wt/vol) bromophenol blue, and 4% 2-mercaptoethanol. The mixtures were then heated at 100°C for 5 min and subjected to SDS/PAGE (12% gels).

Confocal microscopic analyses

CHO-K1 cells, on a glass-bottom 96-well plate (Grainer) at approximately 70% confluency, were incubated for 1 hr with 0.2 μM ER-tracker Red (Invitrogen) and 5 μM dansyl fatostatin. Fluorescent images were captured and analyzed with a Carl Zeiss LSM 510 confocal microscope, equipped with a CSU10 spinning-disk confocal scanner (Yokogawa Electric Corporation) and an ORCA-CCD camera (Hamamatsu Photonics). Images were analysed with IPLab software (Solution Systems).

Binding assays

The membrane fraction of cell lysates was extracted with PBS containing 0.1% FOS-Choline 10 (Hampton Research). The extract was mixed with Neutravidine-agarose beads (10 μL) saturated with biotinylated fatostatin, and incubated for 1 hr. The bound proteins were washed four times with PBS containing 0.1% FOS-Choline 10, boiled in 25 μL of SDS sample buffer, and subjected to western blotting. For the competition assay, saturated amounts of cholesterol or fatostatin were added to the membrane extract before incubating with the beads.

Photocrosslinking assays

On day 0, 293T cells were plated out onto a 100 mm dish. On day 2, the cells were transiently co-transfected with pCMV-SCAP-FLAG, pCMV-SCAP(1-415)-FLAG, pCMV-SCAP(1-448)-FLAG, pCMV-SCAP(1-767)-FLAG or pCMV-SCAP(732-1276)-FLAG using FuGENE 6 reagent (Roche Applied Science). On day 3, the cells were harvested, and

FLAG-tagged full-length SCAP and fragments of SCAP proteins were immunoprecipitated with 20 μg of anti-FLAG IgG-M2 as described below. The pellets were then resuspended 50 μM of conjugate **5** in 100 μL of Nonidat P-40 lysis buffer, incubated for 0.5 hr, and washed for 0.5 hr with 100 μL of Nonidat P-40 lysis buffer. The beads were irradiated using a UV illuminator (UV Transilluminator, UVP) for 10 min (365 nm for 2.5 min then 302 nm for 2.5 min, for a total of two sequences), mixed with 5× SDS loading buffer, and boiled for 5 min. The obtained proteins were subjected to SDS-PAGE and western blot analysis with streptavidin-HRP conjugate and anti-FLAG IgG-M2.

Coimmunoprecipitation of INSIG-1 with SCAP

On day 0, CHO-K1 cells were plated out onto a 100 mm dish of medium A. On day 2, the cells were transiently co-transfected with pTK-HSV-SREBP-2, pCMV-SCAP and pCMV-INSIG-1-Myc (Yang et al., 2002; Yabe et al., 2002) using FuGENE 6 reagent. On day 3, the cells were washed with PBS, and then incubated in medium B in the absence or presence of fatostatin (20 μM) or sterols (10 μg/mL cholesterol and 1 μg/mL 25-hydroxycholesterol). On day 4, the cells were washed once with cold PBS, and then suspended in 1 mL of Nonidat P-40 lysis buffer containing 50 mM Hepes-KOH (pH 7.4), 100 mM NaCl, 1.5 mM $MgCl_2$, 0.1% (vol/vol) Nonidet P-40, and protease inhibitor mixture (1 μg/mL pepstatin A, 10 μg/mL leupeptin, and 2 μg/mL aprotinin) in the absence or presence of fatostatin (20 μM) or sterols (10 μg/mL cholesterol and 1 μg/mL 25-hydroxycholesterol). The cells were lysed by passing through a 22-gauge needle 15 times, and extracted for 1 hr at 4°C. The cell extracts were clarified by centrifugation at $10^5 \times g$

for 30 min. The supernatant was precleared for 1 hr by rotation with 50 μL of Protein G-Sepharose beads (GE Healthcare UK Ltd.). Precleared lysates were rotated for 16 hrs at 4°C, with 20 μg of monoclonal anti-Myc IgG-9E10 together with 50 μL of protein G Sepharose beads. After centrifugation the pelleted beads were washed for 15 min at 4°C with 1 mL of Nonidat P-40 lysis buffer, in the absence or presence of fatostatin (20 μM) or sterols (10 μg/mL cholesterol and 1 μg/mL 25-hydroxycholesterol) four times. The pellets were then resuspended in 100 μL of buffer containing 10 mM Tris-HCl (pH 7.4), 100 mM NaCl, 1% (wt/vol) SDS, and protease inhibitor mixture (1 μg/mL pepstatin A, 10 μg/mL leupeptin, and 2 μg/mL aprotinin) and mixed with 5× SDS loading buffer containing 150 mM Tris-HCl (pH 6.8), 15% SDS, 25% (vol/vol) glycerol, 0.02% (wt/vol) bromophenol blue, and 12.5% (vol/vol) 2-mercaptoethanol. The pellets were boiled for 5 min, and subjected to SDS-PAGE and western blot analysis with IgG-9D5 (SCAP) and IgG-9E10 (INSIG-1).

Animal studies procedures

Four– to five–week-old homozygous male obese (*ob/ob*) mice (C57BL/6J, The Jackson Laboratory, Bar Harbor, ME) were housed under controlled conditions (12 hrs light/dark cycle; 25°C) in the Animal Care Center at Baylor College of Medicine. Animal experiments were conducted in accordance with the Guide for the Care and Use of Laboratory Animals (NIH Publication No. 85-23, revised 1996). The animals were housed 5 per cage, and had *ad libitum* access to standard laboratory chow (Purina Mills, Richmond,

IN) and water for one week after their arrival. On day 1 of the experiment, and every day thereafter, the weight and the amount of food intake of each mouse were measured between 3:00 and 5:00 p.m. The treated mice then received an ip injection of fatostatin (30 mg/kg; 150 μL) while the control mice received 10% DMSO in PBS. Daily injections were continued for 28 days, when the study was ended.

Blood constituents

After 28 days, fatostatin mice were fasted for 5-6 hrs, whole blood glucose and β-hydroxybutyrate were measured with a Glucometer Precision Xtra (Abbott). Measurements of the serum constituents glucose, TG, and cholesterol were performed by the Comparative Pathology Laboratory (Baylor College of Medicine). Serum non-esterified fatty acids (NEFA) were measured using a NEFA C kit (Wako Chemicals, Richmond, VA).

Liver analyses

Mice were sacrificed, and the weights of livers and epididymal fat pads were determined. Frozen sections of liver slices from individual animals were stained with Oil Red O, to visualize the fat droplet—TGs—as previously described (Abu-Elheiga et al., 2001). The remaining liver tissues were frozen in liquid nitrogen and kept at –80°C for further analyses.

Tissue triglyceride and cholesterol contents

Liver triglyceride and cholesterol contents were determined as described by Chandler et al. (2003), using a Cholesterol E Kit (Wako) and an Infinity Triglyceride Kit (Thermo Electron, Melbourne, Australia).

Enzymatic activities and western blot analyses

A portion of the frozen liver was ground to powder in liquid nitrogen. The powder was suspended in 10 mL of PBS containing 0.1 mM PMSF, 5 mM benzamidine, and 5 mg/mL protease inhibitor cocktail (Roche), and then homogenized using Polytron (3 × 30 sec, at high speed) and sonicated briefly to degrade DNA. The extracts were clarified by centrifugation at 16,000 × g for 20 min. Protein concentrations in the supernatant were determined, and subjected to western blot analysis using antibodies against FAS, ACC, SCD1 and ACL. The intensities of the specific bands of proteins of interest were scanned and normalized against β-actin for quantifications. FAS and ACC activities from the liver extracts were determined as described earlier (Mao et al., 2006).

ACKNOWLEDGMENTS

This work was supported in part by grants to M.U. from the U.S. Department of Defense Prostate Cancer Research Program, the Suzuken Memorial Foundation, Kato Memorial Bioscience Foundation, and MEXT (Grant-in-Aid 18390002), and by grants to S.J.W. from the Hefni Technical Training Foundation and the National Institutes of Health (GM-63115). We thank Dr. William C. Heird, Department of Pediatrics, Children's Nutrition Research Center, for conducting the fatty acid analyses. We also thank T. Orihara, T. Morii, and T. Hasegawa for encouragement and experimental support. S.K. is a postdoctoral fellow of JSPS. The Kyoto research group participates in the Global COE program "Intergrated Materials Science" (#B-09). The upgrade of the confocal microscope was supported by NEDO and Yokogawa Electric Corporation.

REFERENCES

Abu-Elheiga, L., Matzuk, M.M., Abo-Hashema, K.A., and Wakil, S.J. (2001). Continuous fatty acid oxidation and reduced fat storage in mice lacking acetyl-CoA carboxylase 2. Science *291*, 2613-2616.

Abu-Elheiga, L., Oh, W., Kordari, P. and Wakil, S.J. (2003). Acetyl-CoA carboxylase 2 mutant mice are protected against obesity and diabetes induced by high-fat/high-carbohydrate diets. Proc. Natl. Acad. Sci. USA *100*, 10207-10212.

Adams, C.M., Reitz, J., De Brabander, J.K., Feramisco, J.D., Li, L., Brown, M.S. and Goldstein, J.L. (2004). Cholesterol and 25-hydroxycholesterol inhibit activation of SREBPs by different mechanisms, both involving SCAP and Insigs. J. Biol. Chem. *279*, 52772–52780

Brown, M.S., and Goldstein, J.L. (1997). The SREBP pathway: regulation of cholesterol metabolism by proteolysis of a membrane-bound transcription factor. Cell *89*, 331-340.

Cho, M.C., Lee, K., Paik, S.G., and Yoon, D.Y. (2008). Peroxisome proliferators-activated receptor (PPAR) modulators and metabolic disorders. PPAR research *2008*, 679137

Choi, Y., Kawazoe, Y., Murakami, K., Misawa, H., and Uesugi, M. (2003). Identification of bioactive molecules by adipogenesis profiling of organic compounds. J. Biol. Chem. *278*, 7320-7324.

DeBose-Boyd, R.A., Brown, M.S., Li, W.P., Nohturfft, A., Goldstein, J.L., and Espenshade, P.J. (1999). Transport-dependent proteolysis of SREBP: relocation of site-1 protease from Golgi to ER obviates the need for SREBP transport to Golgi. Cell *99*, 703-712.

Du, X., Kristiana, I., Wong, J., and Brown, A.J. (2006). Involvment of Akt in ER-to-Golgi Transport of SCAP/SREBP: A link between a key cell proliferative pathway and membrane synthesis. Mol. Biol. Cell *17*, 2735-2745

Espenshade, P.J., Li, W.P. and Yabe, D. (2002). Sterols block binding of COPII proteins to SCAP, thereby controlling SCAP sorting in ER. Proc. Natl. Acad. Sci. USA *99*, 11694-11699.

Gibbons, G.F. (2003). Regulation of fatty acid and cholesterol synthesis: co-operation or competition? Progress in Lipid Research *42*, 479-497.

Goldstein, J.L., DeBose-Boyd, R.A., and Brown, M.S. (2006). Protein sensors for membrane sterols. Cell *124*, 35-46.

Grand-Perret, T., Bouillot, A., Perrot, A., Commans, S., Walker, M., and Issandou, M. (2001). SCAP ligands are potent new lipid-lowering drugs. Nat. Med. *7*, 1332-1338.

Horton, J.D., Shah, N.A., Warrington, J.A., Anderson, N.N., Park, S.W., Brown, M.S., and Goldstein, J.L. (2003). Combined analysis of oligonucleotide microarray data from transgenic and knockout mice identifies direct SREBP target genes. Proc. Natl. Acad. Sci. USA *100*, 12027-12032.

Horton, J.D., Shimomura, I., Ikemoto, S., Bashmakov, Y., and Hammer, R.E. (2003). Overexpression of sterol regulatory element-binding protein-1a in mouse adipose tissue produces adipocyte hypertrophy, increased fatty acid secretion, and fatty liver. J. Biol. Chem. *278*, 36652-36660.

Hua, X., Sakai, J., Ho, Y.K., Goldstein, J.L., and Brown, M.S. (1995). Hairpin orientation of sterol regulatory element-binding protein-2 in cell membranes as determined by protease protection. J. Biol. Chem. *270*, 29422-29427.

Hua, X., Nohturfft, A., Goldstein, J.L., and Brown, M.S. (1996). Sterol resistance in CHO cells traced to point mutation in SREBP cleavage-activating protein. Cell *87*, 415-426.

Ide, T., Shimano, H., Yahagi, N., Matsuzaka, T., Nakakuki, M., Yamamoto, T., Nakagawa, Y., Takahashi, A., Suzuki, H., Sone, H., et al. (2004). SREBPs suppress IRS-2-mediated insulin signalling in the liver. Nat. Cell Biol. *6*, 351-357.

Mao, J., DeMayo, F.J., Li, H., Abu-Elheiga, L., Gu, Z., Shaikenov, T.E., Kordari, P., Chirala, S.S., Heird, W.C., and Wakil, S.J. (2006). Liver-specific deletion of acetyl-CoA carboxylase 1 reduces hepatic triglyceride accumulation without affecting glucose homeostasis. Proc. Natl. Acad. Sci. USA *103*, 8552-8557.

Nohturfft, A., Brown, M.S., and Goldstein, J.L. (1998). Sterols regulate processing of carbohydrate chains of wild-type SREBP cleavage-activating protein (SCAP), but not sterol-resistant mutants Y298C or D443N. Proc. Natl. Acad. Sci. USA *95*, 12848-12853.

Oh, W., Abu-Elheiga, L., Kordari, P., Gu, Z., Shaikenov, T., Chirala, S.S. and Wakil, S.J. (2005). Glucose and fat metabolism in adipose tissue of acetyl-CoA carboxylase 2 knockout mice. Proc. Natl. Acad. Sci. USA *102*, 1384-1389.

Osborne, T.F. (2000). Sterol regulatory element-binding proteins (SREBPs): key regulators of nutritional homeostasis and insulin action. J. Biol. Chem. *275*, 32379-32382.

Radhakrishnan, A., Sun, L.P., Kwon, H.J., Brown, M.S., and Goldstein, J.L. (2004). Direct binding of cholesterol to the purified membrane region of SCAP: mechanism for a sterol-sensing domain. Mol. Cell *15*, 259-268.

Sakai, J., Duncan, E.A., Rawson, R.B., Hua, X., Brown, M.S., and Goldstein, J.L. (1996). Sterol-regulated release of SREBP-2 from cell membranes requires two sequential cleavages, one within a transmembrane segment. Cell *85*, 1037-1046.

Sakai, J., Rawson, R.B., Espenshade, P.J., Cheng, D., Seegmiller, A.C., Goldstein, J.L., and Brown, M.S. (1998). Molecular identification of the sterol-regulated luminal protease that cleaves SREBPs and controls lipid composition of animal cells. Mol. Cell *2*, 505-514.

Sakai, J., Nohturfft, A., Goldstein, J.L., and Brown, M.S. (1998). Cleavage of sterol regulatory element-binding proteins (SREBPs) at site-1 requires interaction with SREBP cleavage-activating protein. J. Biol. Chem. *273*, 5785–5793

Sato, R., Yang, J., Wang, X., Evans, M.J., Ho, Y.K., Goldstein, J.L., and Brown, M.S. (1994). Assignment of the membrane attachment, DNA binding, and transcriptional activation domains of sterol regulatory element binding protein-1 (SREBP-1). J. Biol. Chem. *269*, 17267–17273.

Sato, S., Kwon, Y., Kamisuki, S., Srivastava, N., Mao, Q., Kawazoe, Y., and Uesugi, M. (2007). Polyproline-rod approach to isolating protein targets of bioactive small molecules: isolation of a new target of indomethacin. J. Am. Chem. Soc. *129*, 873-880.

Wakil, S.J. (1989). The fatty acid synthase: A proficient multifunctional enzyme. Biochemistry *28*, 4523-4530.

Yabe, D., Brown, M.S., and Goldstein, J.L. (2002). Insig-2, a second endoplasmic reticulum protein that binds SCAP and blocks export of sterol regulatory element-binding proteins. Proc. Natl. Acad. Sci. USA *99*, 12753-12758.

Yahagi, N., Shimano, H., Hasty, A.H., Matsuzaka, T., Ide, T., Yoshikawa, T., Amemiya-Kudo M., Tomita, S., Okazaki, H., Tamura, Y., et al. (2002). Absence of sterol regulatory element-binding protein-1 (SREBP-1) ameliorates fatty livers but not obesity or insulin resistance in Lep(ob)/Lep(ob) mice. J. Biol. Chem. *277*, 19353-19357.

Yang, J., Brown, M.S., Ho, Y.K., and Goldstein, J.L. (1995). Three different rearrangements in a single intron truncate sterol regulatory element binding protein-2 and produce sterol-resistant phenotype in three cell lines. Role of introns in protein evolution. J. Biol. Chem. *270*, 12152-12161.

Yang, T., Espenshade, P.J., Wright, M.E., Yabe, D., Gong, Y., Aebersold, R., Goldstein, J.L., and Brown, M.S. (2002). Crucial step in cholesterol homeostasis: sterols promote binding of SCAP to INSIG-1, a membrane protein that facilitates retention of SREBPs in ER. Cell *110*, 489-500.

Ye, J., Rawson, R.B., Komuro, R., Chen, X., Davé, U.P., Prywes, R., Brown, M.S., and Goldstein, J.L. (2000). ER stress induces cleavage of membrane-bound ATF6 by the same proteases that process SREBPs. Mol. Cell *6*, 1355-1364.

FIGURE LEGENDS

Figure 1. Fatostatin blocks activation of SREBP

(A) Structure of fatostatin. (B) Downregulation of affected genes confirmed by RT-PCR. DU145 cells were treated with DMSO (lane 1) or 5 μM fatostatin (lane 2) for 6 h. Total RNA was then extracted and subjected to RT-PCR for ATP citrate lyase (ACL), 3-hydroxy-3-methyl-glutaryl-CoA reductase (HMG-CoAR), low-density lipoprotein receptor (LDLR), mevalonate pyrophosphate decarboxylase (MVD), stearoyl-CoA desaturase (SCD1), insulin-induced gene 1 (INSIG-1), and glyceraldehyde-3-phosphate dehydrogenase (GAPDH). (C) Decrease in selected genes, shown in microarray analyses and confirmed by decreases in their RT-PCR measurements, caused by treatment with fatostatin. (D) Suppression by fatostatin of ability of endogenous SREBPs to activate transcription of reporter gene. CHO-K1 cells were transfected with a reporter gene, in which the expression of luciferase was controlled by three repeats of sterol-responsive elements (SREs) (pSRE-Luc) and treated by varied concentrations of fatostatin in a medium containing lipid-free serum. (E) Effect of fatostatin (20 μM) on CHO-K1 cells co-transfected with pCMV-SREBP-1c(1-436) and pSRE-Luc in a medium containing lipid-free serum. (F) PLAP-BP2 in transfected CHO-K1 cells remains membrane-bound, unless it is cleaved by S1P in the Golgi apparatus and secreted into the culture medium. Compared with EtOH controls, treatment with fatostatin (20 μM) or sterols (10 μg/mL cholesterol and 1 μg/mL 25-hydroxycholesterol) affects cleavage of PLAP-BP2. (G) Western blot analysis

of CHO-K1 cells treated with fatostatin. *P* and *N* denote the uncleaved membrane precursor and cleaved active nuclear forms of SREBP-2, respectively.

Figure 2. Fatostatin blocks translocation of SREBPs from ER to Golgi

(A) Western blot analysis showing effects of brefeldin A (1 μg/mL) on CHO-K1 cells treated with EtOH alone, or EtOH containing fatostatin (20 μM), or sterols (10 μg/ml cholesterol and 1 μg/ml 25-hydroxycholesterol). (*P* and *N* are defined in the Figure 1 legend.) (B) SCAP contains a glycosylated luminal loop, which is protected from proteolysis by trypsin and which recognizes anti-SCAP IgG-9D5. When SCAP resides in the ER, the two oligosaccharides in the loop are sensitive to endoglycosidase H. As SCAP is transported to the Golgi apparatus, its sugars become resistant to digestion by endoglycosidase H. (C) Western blot analysis with anti-SCAP IgG-9D5 of cells grown in the absence or presence of fatostatin (20 μM) or sterols (10 μg/mL cholesterol and 1 μg/mL 25-hydroxycholesterol). Numbers on the right denote the number of N-linked sugar chains present on protease-protected SCAP fragments.

Figure 3. Fatostatin interacts with SCAP

(A) The structures of dansyl fatostatin and fatostatin-polyproline linker-biotin conjugate. The polyproline linker was inserted for better projection of the fatostatin molecule (Sato et al., 2007). (B) CHO-K1 cells treated with dansyl fatostatin and ER-tracker red showing localization of dansyl fatostatin in the ER. Scale bar = 10 μm. (C) Interaction of fatostatin-

polyproline linker-biotin conjugate **3** with SCAP. Proteins bound to Neutravidine-agarose beads saturated with fatostatin-polyproline linker-biotin conjugate **3** were isolated from CHO-K1 membrane extracts, and then analyzed by western blots with anti-SCAP, anti-SREBP-1, anti-SREBP-2, anti-HMG-CoAR, and anti-ATF6 antibodies. SCAP was the only protein that interacted with conjugate **3**. Control experiments with polyproline linker-biotin conjugate **4** that did not contain fatostatin gave negative results. (D) For the competition assay, membrane extracts were preincubated with EtOH alone, cholesterol, or fatostatin.

Figure 4. Direct interaction of fatostatin with SCAP

(A) The structure of conjugate **5**. (B) Conjugate **5**-crosslinked proteins. FLAG-tagged full-length SCAP (amino acids 1-1276) and fragments of SCAP (amino acids 1-415, 1-448, 1-767 and 732-1276) proteins were expressed in 293T cells and immunoprecipitated with a FLAG antibody. Conjugate **5**-crosslinked proteins were detected by streptavidin-HRP (left) or a FLAG antibody (right). The asterisk denotes a FLAG antibody used for the immunoprecipitation.

Figure 5. Coimmunoprecipitation of INSIG-1 with SCAP

CHO-K1 cells expressing Myc-tagged INSIG-1 were treated with EtOH alone, or EtOH containing fatostatin (20 μM), or sterols (10 μg/ml cholesterol and 1 μg/ml 25-hydroxycholesterol). The cells were harvested, lysed, and immunoprecipitated with anti-Myc antibody to precipitate INSIG-1. Pellets were subjected to western blot analysis with anti-SCAP and anti-Myc antibodies.

Figure 6. Effects of fatostatin on body weight, food consumption, and blood constituents of male *ob/ob* mice

(A) Representative control and fatostatin-treated mice. (B) Weight and cumulative food intake per mouse during 28 days treatment. (C) Blood constituents of control and fatostatin-treated mice following treatment for 28 days (mean ± SD, $n = 5$, * $p < 0.05$).

Figure 7. Effects of fatostatin on liver and adipose tissue of *ob/ob* mice

(A) Representative livers of the fatostatin-treated and control mice. (B) The weight of livers and epididymal fat pads from fatostatin-treated and control mice (mean ± SD, $n = 5$, $^{*}P < 0.05$). (C) Sections of the livers of fatostatin-treated and control mice showing Oil Red-O stained lipid droplets. (D) TGs and cholesterol levels in the livers of fatostatin-treated and control mice (mean ± SD, $n = 5$, * $p = 0.0004$, † $p = 0.03$). (E) Activity of ACC and FAS were measured in liver extracts of *ob/ob* mice (mean ± SD, $n = 5$, $^{\dagger}P = 0.005$, $^{\ddagger}P = 0.002$). (F) Western Blot analysis of liver crude extracts. (G) Ratio of intensity of specific bands of different lipogenic enzymes from fatostatin against control mice after normalization to actin (mean ± SD, $n = 5$, $^{*}P < 0.05$). (H) Relative levels of mRNA of lipogenic enzymes in livers of fatostatin-treated and control *ob/ob* mice. RNA was isolated from both the fatostatin-treated mice (n = 5) and the control mice (n = 5) and measured by real-time RT-PCR, as described earlier (Oh et al., 2005). The values were normalized to actin ($^{*}P < 0.05$).

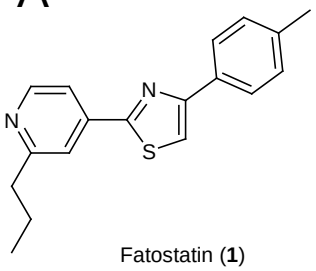

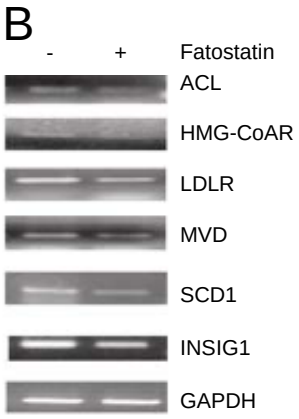

C

Fold decreased

	Microarray	RT-PCR
ACL	0.57	0.47
HMG-CoAR	0.47	0.54
LDLR	0.62	0.58
MVD	0.33	0.50
SCD1	0.57	0.47
INSIG1	0.33	0.64
GAPDH	1.00	0.92

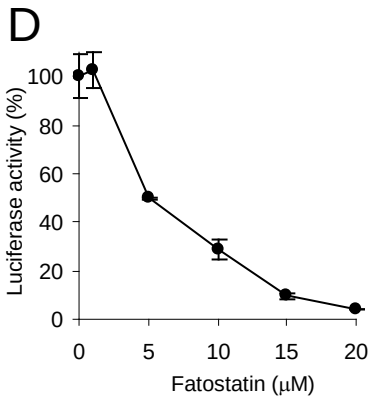

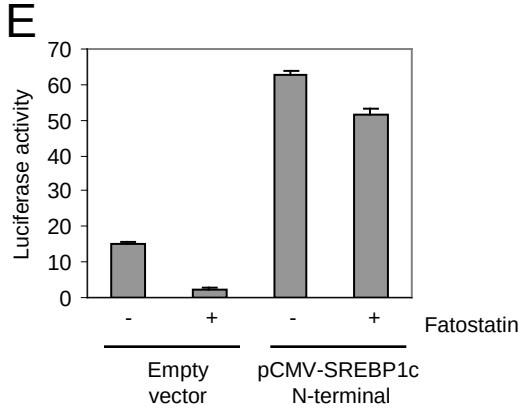

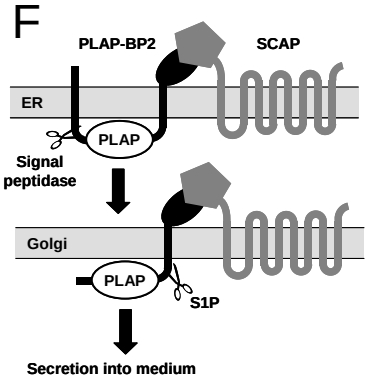

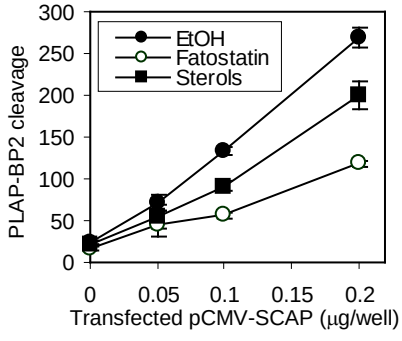

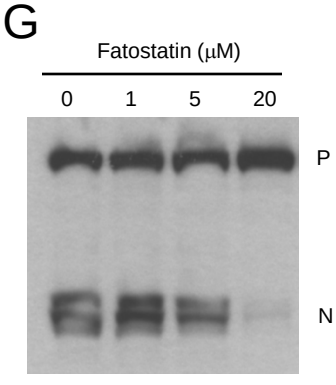

Figure 1

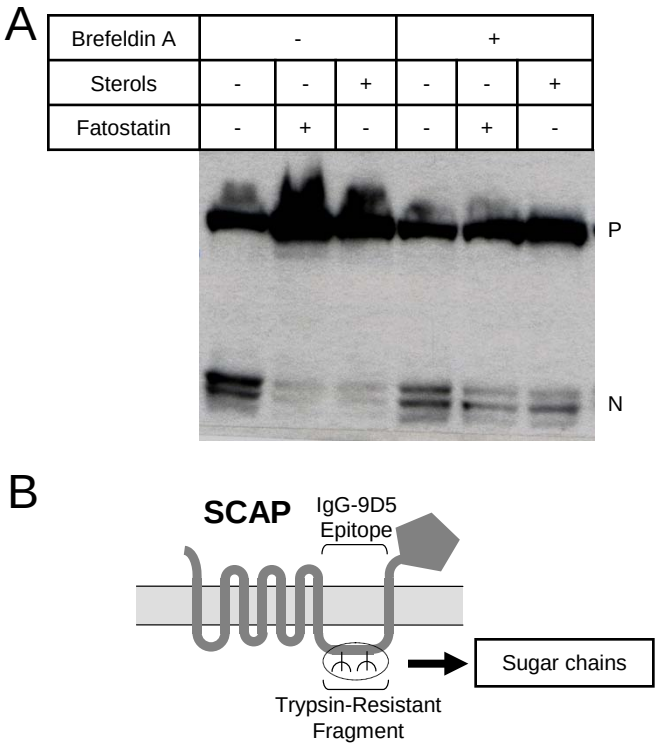
A
Brefeldin A
-
+
Sterols
- - + - - +
Fatostatin
- + - - + -
P
N
B
SCAP
IgG-9D5
Epitope
Sugar chains
Trypsin-Resistant
Fragment
C
Sterols
- - +
Fatostatin
- + -
2
1
0
No. of
Sugar
Chains

Figure 2

A

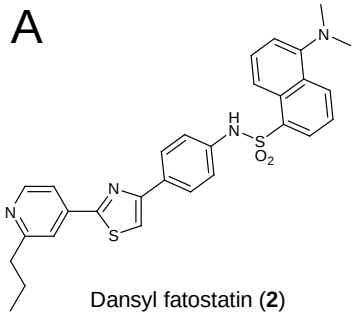

Dansyl fatostatin (**2**)

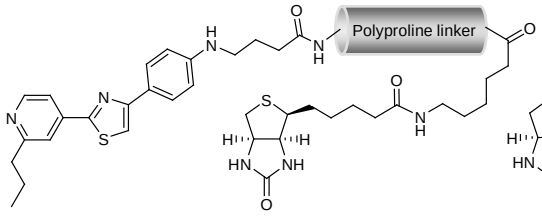

Fatostatin-polyproline linker-biotin conjugate (**3**)

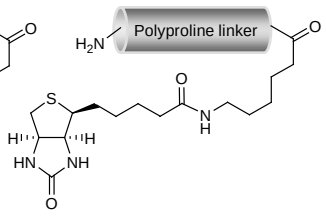

Polyproline linker-biotin conjugate (**4**)

B

C

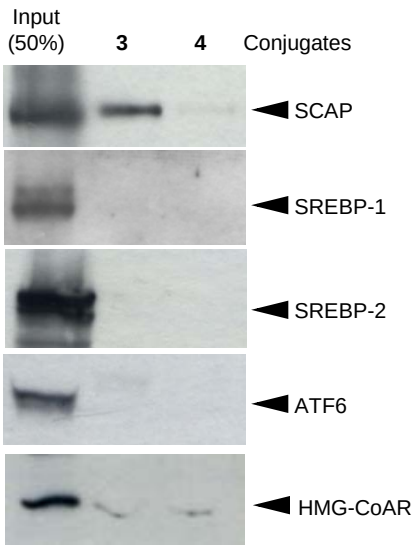

D

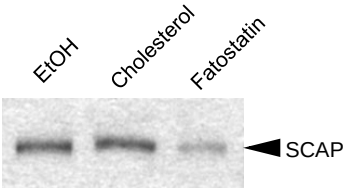

Figure 3

A

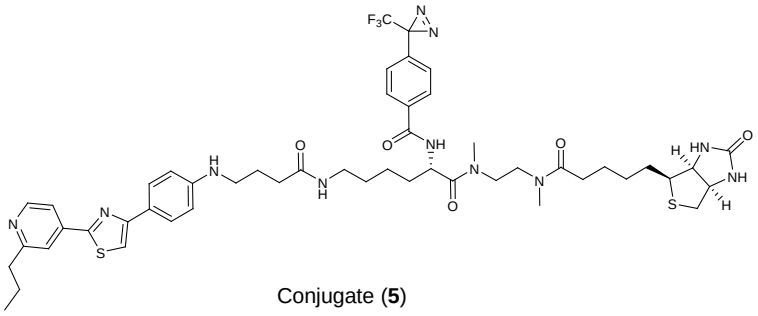

Conjugate (**5**)

B

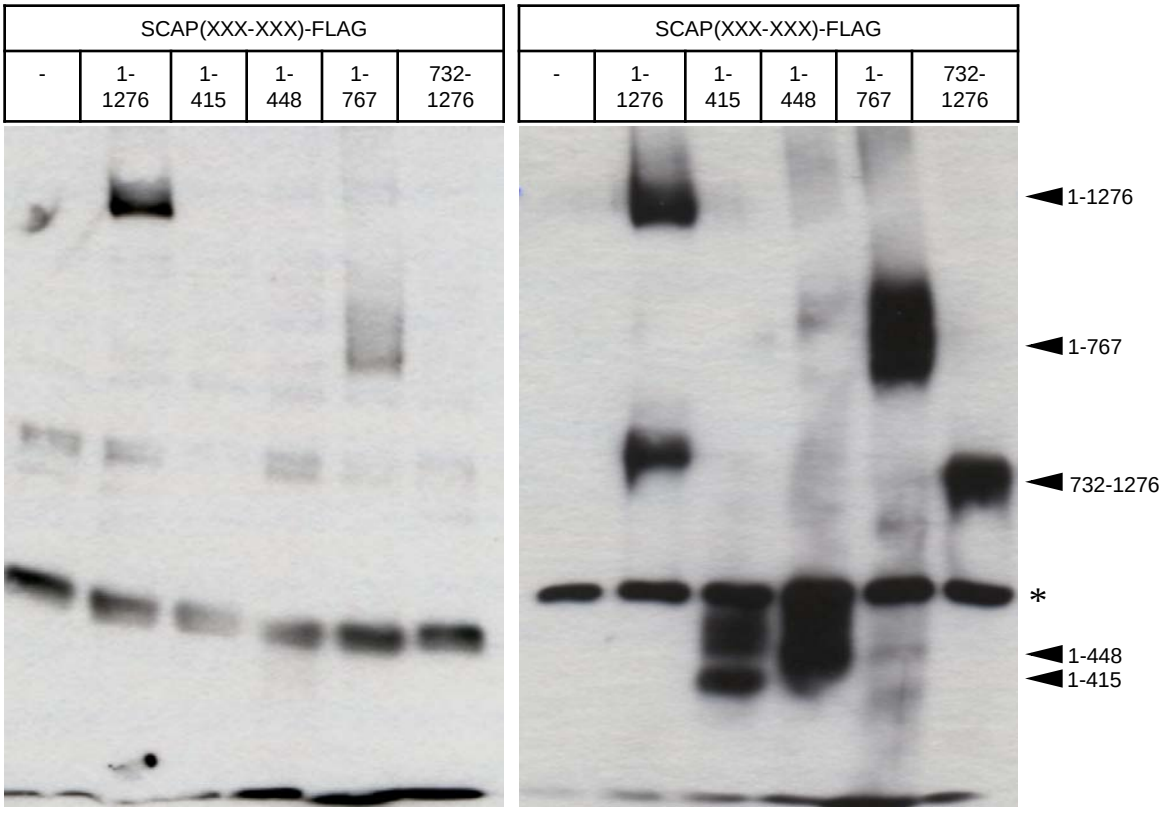

Streptavidin-HRP

Anti-FLAG

Figure 4

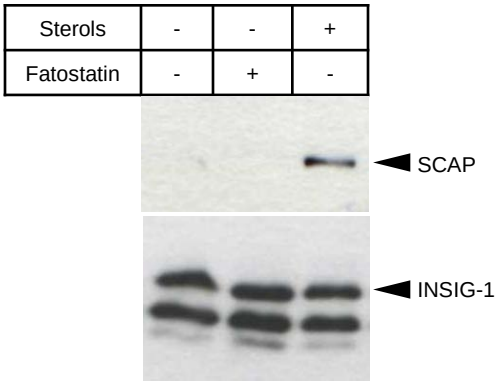

IP: INSIG-1

Figure 5

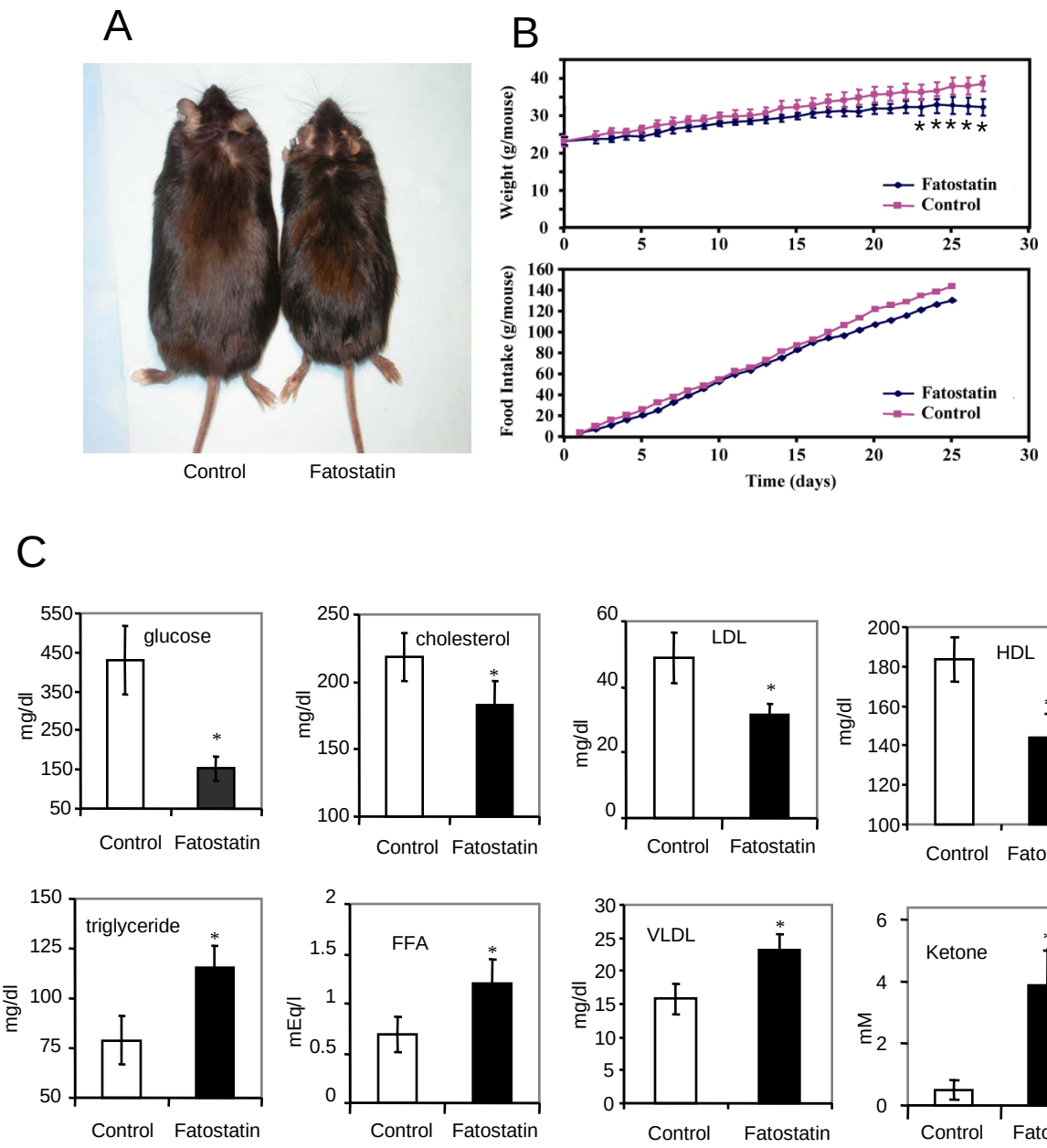
A
Control
Fatostatin
B
Weight (g/mouse)
*****
Fatostatin
Control
Food Intake (g/mouse)
Fatostatin
Control
Time (days)
C
glucose
mg/dl
Control
Fatostatin
cholesterol
mg/dl
Control
Fatostatin
LDL
mg/dl
Control
Fatostatin
HDL
mg/dl
Control
Fatostatin
triglyceride
mg/dl
Control
Fatostatin
FFA
mEq/l
Control
Fatostatin
VLDL
mg/dl
Control
Fatostatin
Ketone
mM
Control
Fatostatin

Figure 6

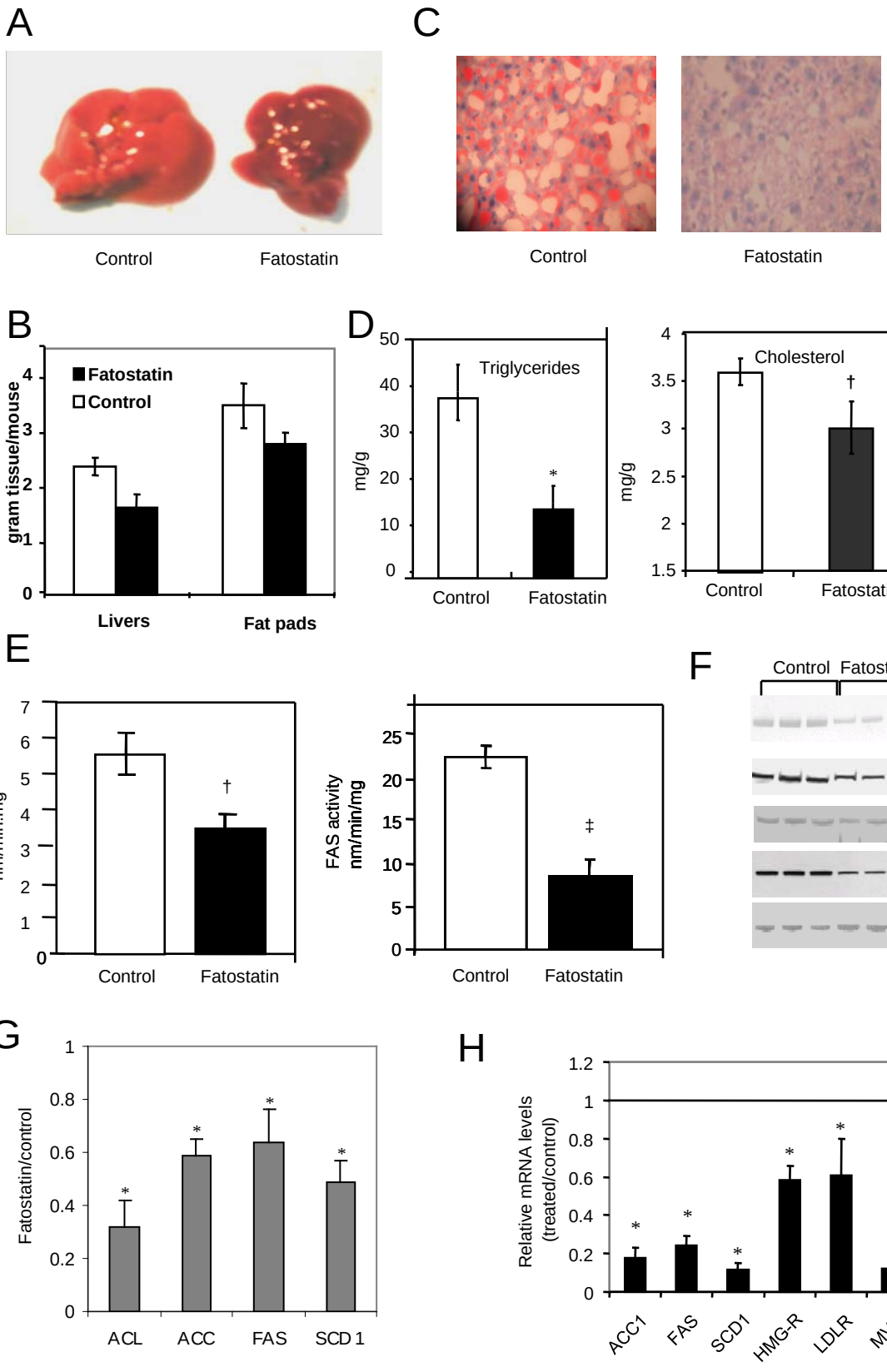
A
Control
Fatostatin
C
Control
Fatostatin
B
Fatostatin
Control
gram tissue/mouse
Livers
Fat pads
D
Triglycerides
mg/g
Control
Fatostatin
Cholesterol
mg/g
Control
Fatostatin
E
ACC activity
nm/min.mg
Control
Fatostatin
FAS activity
nm/min/mg
Control
Fatostatin
F
Control
Fatostatin
FAS
ACC
SCD1
ACL
Actin
G
Fatostatin/control
ACL
ACC
FAS
SCD 1
H
Relative mRNA levels
(treated/control)
ACC1
FAS
SCD1
HMG-R
LDLR
MVD

Figure 7